

The W.R. Wiley Environmental Molecular Sciences Laboratory (EMSL) is a U.S. Department of Energy (DOE) national scientific user facility located at Pacific Northwest National Laboratory (PNNL) in Richland, Washington. EMSL is operated by PNNL for the DOE Office of Biological and Environmental Research. At one location, EMSL offers a comprehensive array of leading-edge resources in six research facilities.

Access to the capabilities and instrumentation in EMSL facilities is obtained on a peer-reviewed proposal basis, and users are participants on accepted proposals. EMSL staff members work with users to expedite access to the research facilities, support capabilities, and the resident scientific expertise. The bimonthly report documents research and activities of EMSL staff and users.

## Research Highlights

### Study of Martensitic Phase Transformation in a NiTiCu Thin-Film Shape-Memory Alloy Using Photoelectron Emission Microscopy

*JM Cai,<sup>(a)</sup> SC Langford,<sup>(a)</sup> M Wu,<sup>(b)</sup> W Huang,<sup>(b)</sup> G Xiong,<sup>(c)</sup> TC Droubay,<sup>(c)</sup> AG Joly,<sup>(c)</sup> KM Beck,<sup>(d)</sup> WP Hess,<sup>(c)</sup> and JT Dickinson<sup>(a)</sup>*

*(a) Washington State University, Pullman, Washington*

*(b) Technological University, Republic of Singapore*

*(c) Pacific Northwest National Laboratory, Richland, Washington*

*(d) W.R. Wiley Environmental Molecular Sciences Laboratory, Richland, Washington*

*This work describes a unique imaging instrument for characterizing the spatial and temporal changes in the phases and microstructures on the surfaces of a wide variety of materials, including shape-memory alloys. Understanding how changes in microstructure affects the electronic properties of a material may enable creation of novel materials with unique electrical and optical properties.*

Shape-memory alloys (SMAs) are an important class of intelligent materials, with properties that can be programmed to achieve specific mechanical responses. When mechanically or thermally cycled, SMAs exhibit reversible shape changes that are associated with a solid-state, martensitic phase transformation. The development of new SMAs is being driven by market demands, especially in micro-electromechanical systems. Recently, SMA thin films have been investigated for applications in microsensors and microactuators. Phase transformations in SMA thin films are often accompanied by significant changes in mechanical, physical, chemical, electrical, and optical properties, including yield stress, elastic modulus, damping modulus, hardness, electrical resistivity, thermal conductivity, thermal expansion, and surface roughness.

Martensitic phase transformations are diffusionless, first-order transformations that involve shear deformation. The thermal responses of bulk SMAs typically are studied using differential scanning calorimetry, which exploits the exothermic/endergonic character of the phase transformation. This technique does not provide information on the associated microstructure. On the other hand, photoelectron emission microscopy (PEEM) exploits photoelectron emission to image the surface. Photoelectron emission depends strongly on the work function of the imaged surface, which in turn depends strongly on a materials microstructure. Thus, martensitic phase transformations can significantly alter the electronic and optical properties of SMAs. For this reason, we employed *in situ* PEEM to characterize the transformation of a thin film of NiTiCu SMA in real time.

PEEM images of the SMA film at 25°C (martensite phase) and at 100°C (austenite phase) are shown in Figure 1. The most prominent difference between the images is the presence of wrinkle-like features on the surface of the low-temperature phase in Figure 1a, and the absence of these features on the surface of the high-temperature phase in Figure 1b. Sequences of PEEM images acquired while cycling the temperature indicate that the wrinkles disappear at 73.1°C during heating and reappear at 52.4°C during cooling under the conditions of this work.

The wrinkles in the PEEM image of Figure 1a show consistent variation in brightness. In general, the wrinkles are brighter along one edge and darker along the other. The wrinkles in the field of view run predominately from the lower left to the upper right, with the bright edge on the upper left. The magnitude of this variation is indicated in Figure 1c, which displays the PEEM intensity as a function of position along the white line in Figure 1a. These intensity variations are typically interpreted in terms of variations in the sample work function or topography.

Significantly, the PEEM image of the high-temperature phase in Figure 1b is darker than the image of the low-temperature phase in Figure 1a. Quantitative measurements of the integrated image intensities during heating and cooling are plotted in Figure 2. The PEEM intensity is nearly constant from 45 to 70°C, and then decreases monotonically from 70 to 120°C. This decrease corresponds roughly to the temperature range of the phase transformation during heating. During cooling from 120 to 55°C, the photoelectron intensity increases slowly, and then rises rapidly to levels associated with the early stages of heating between 50 and 55°C.

The real-time PEEM images of a NiTiCu SMA film show distinct trenches near room temperature that disappear as the temperature is raised above 73°C. During heating, the image intensities decrease gradually because of a corresponding gradual increase in surface work function. When the film is subsequently cooled, these trenches reappear between 52 and 53°C; near this same temperature, the PEEM image intensities increase suddenly, in concert with a sharp drop in work function. The magnitude of the effective work-function change during thermal cycling is about 0.16 eV. We attribute the sharp change in work function and PEEM intensity during cooling to the rapid transformation of surface material from austenite to martensite.

The surface sensitivity of PEEM measurements reveal correlations between changes in microstructure and electronic structure on time scales of seconds or less with sub-micrometer spatial resolution. These capabilities make PEEM an important tool for characterizing the spatial and temporal changes in phase and

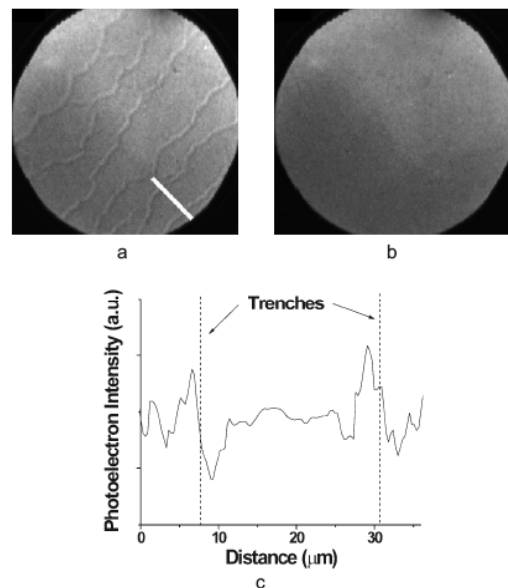


**Figure 1.** *In situ* PEEM images of the NiTiCu thin film at 25°C (a) and 100°C (b). The PEEM intensity along the white line in (a) is shown in (c). The dotted lines in (c) mark the approximate positions of the trenches.

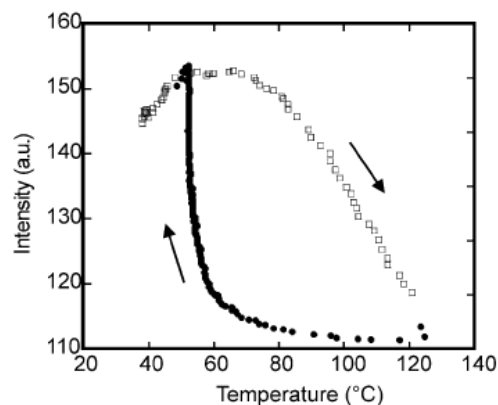


**Figure 2.** Integrated photoelectron intensities versus temperature during heating and cooling of the NiTiCu thin film: solid black dots are for heating, open squares are for cooling, and open circles are for cooling.

microstructure in a wide variety of materials, including SMAs. A paper describing this exciting work was published in the January issue of the *Journal of Advanced Functional Materials*.

### Citation

Cai M, SC Langford, MJ Wu, WM Huang, G Ziong, TC Droubay, AG Joly, KM Beck, WP Hess, and JT Dickinson. 2007. “Use of Martensitic Phase Transition in a NiTiCu Thin Film Shape Memory Alloy Using Photoelectron Emission Microscopy.” *Journal of Advanced Functional Materials* 17(1):161-167.

## Relative Raman Intensities in $C_6H_6$ , $C_6D_6$ , and $C_6F_6$ : A Comparison of Different Computational Methods

SD Williams,<sup>(a)</sup> TJ Johnson,<sup>(b)</sup> TP Gibbons,<sup>(a)</sup> CL Kitchens<sup>(a)</sup>

(a) Appalachian State University, Boone, North Carolina

(b) Pacific Northwest National Laboratory, Richland, Washington

*As supercomputers allow molecular modeling to better model and predict what is observed by experimental scientists, it is important to “reality check” whether the models are in fact true to the data. In this study, various theoretical models were vetted against careful analytical work to determine which programs could best (and how well) model experimental data for a method useful not only to basic science, but also to real-world applications such as environmental monitoring/restoration.*

In this project we compared the accuracy of various computational methods (Hartree-Fock, MP2, CCSD, CAS-SCF, and several types of density functional theory) for predicting relative intensities in Raman spectra for  $C_6H_6$ ,  $C_6D_6$ , and  $C_6F_6$ . The predicted relative intensities for  $\nu_1$  and  $\nu_2$  were compared with relative intensities measured by a Fourier Transform-Raman spectrometer. While none of these methods excelled at this prediction, the Hartree-Fock method using a large basis set was most successful for predictions of  $C_6H_6$  and  $C_6D_6$ , while the PW91PW91 method was the most successful for  $C_6F_6$ . The degree of success can be seen in Figures 1 and 2, where the experimental points are displayed as circles and the solid lines are the fit to the data. A paper based on this work was published in the February issue of *Theoretical Chemistry Accounts*.

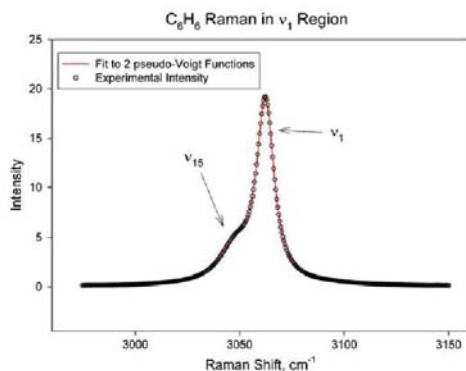


**Figure 1.** Experimental Raman intensities (corrected for spectrometer response) for liquid benzene in the CH stretch region,  $2\text{ cm}^{-1}$  resolution. The solid line is a fit to two pseudo-Voigt lineshapes.  $R_2$  for the fit was 0.9998, and the area for  $\nu_1$  was  $279 \pm 1$ .

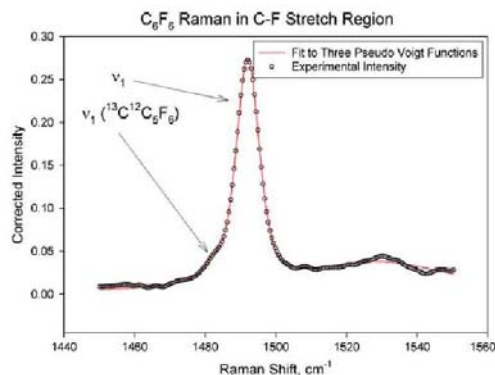


**Figure 2.** Experimental Raman intensities (corrected for spectrometer response) for liquid  $C_6F_6$  in the CF stretch region,  $2\text{ cm}^{-1}$  resolution. The solid line is a fit to three pseudo-Voigt lineshapes.  $R_2$  for the fit was 0.998, and the area for  $\nu_1$  was  $2.7 \pm 0.5$ .

### Citation

Williams SD, TJ Johnson, TP Gibbons, and CLKitchens. 2007. “Relative Raman Intensities in  $C_6H_6$ ,  $C_6D_6$ , and  $C_6F_6$ : A Comparison of Different Computational Methods.” *Theoretical Chemistry Accounts* 117(2):283-290.

## Magnetic Resonance Studies of Proton Loss from Carotenoid Radical Cations

LD Kispert,<sup>(a)</sup> A Ligia Focsan,<sup>(a)</sup> TA Konovalova,<sup>(a)</sup> J Lawrence,<sup>(a)</sup> MK Bowman,<sup>(b)</sup> DA Dixon,<sup>(a)</sup> P Molnar,<sup>(c)</sup> and J Deli<sup>(c)</sup>

(a) University of Alabama, Tuscaloosa, Alabama

(b) Pacific Northwest National Laboratory, Richland, Washington

(c) University of Pécs, Pécs, Hungary

*An important protective process in photosynthetic organisms is the ability to cope with more light energy than can be used for photosynthesis. This excess energy must be dissipated or the chlorophyll (Ch1) will be damaged and cease to function. This protection of chlorophyll often involves carotenoids, but the chemical mechanism is not well known. In this study, we used electron paramagnetic resonance to study the reactive species to determine the pathway through which energy is dissipated.*

Carotenoids are intrinsic components of reaction centers and pigment-protein complexes in photo-synthetic membranes and play a photoprotective role and serve as a secondary electron donor. The robust nature of carotenoids in living materials requires extensive characterization of their electron-transfer mechanism, radical-trapping ability, stability, structure in and on various hosts, and photochemical behavior before optimum use of them can be made in artificial photosynthetic systems.

In this project, we employed a combination of pulsed electron nuclear double resonance (ENDOR) spectrometry, two-dimensional hyperfine sublevel correlation spectroscopy (2D-HYSCORE) using the electron paramagnetic resonance (EPR) equipment available in EMSL, and density functional theory (DFT) calculations to study this system. This combined experimental/computational approach revealed that photo-oxidation of natural zeaxanthin (I) and violaxanthin (II) on silica-alumina produces not only the carotenoid radical cations ( $\text{Car}^{\bullet+}$ ) but also neutral radicals ( $\# \text{Car}^{\bullet}$ ) by proton loss from the methyl groups at positions 5 or 5', and possibly positions 9 or 9' and 13 or 13'. Notably, the proton loss favored in I at position 5 by DFT calculations, is unfavorable in II because of the epoxide at the 5, 6 position. Density function theory calculations predict the isotropic methyl proton couplings of 8 to 10 MHz for  $\text{Car}^{\bullet+}$ , which agree with the ENDOR data for carotenoid  $\pi$ -conjugated radical cations. Large  $\alpha$ -proton hyperfine coupling constants ( $> 10$  MHz) determined from HYSCORE are assigned from the DFT calculations to neutral carotenoid radicals. Proton loss upon photolysis was also examined as a function of carotenoid polarity [Lycopene (III) versus 8'-apo- $\beta$ -caroten-8'-al (IV)]; hydrogen bonding [Lutein (V) versus III]; host [silica-alumina versus MCM-41 molecular sieve]; and substituted metal in MCM-41.

Loss of  $\text{H}^+$  from the 5(5'), 9(9'), or 13(13') methyl positions has importance in photoprotection. Photoprotection involves non-photochemical quenching in which  $^1\text{Ch1}^*$  decays via 1) energy transfer to the carotenoid, which returns to the ground state by thermal dissipation, or 2) electron transfer to form a charge transfer state ( $\text{I}^{\bullet+} \cdots \text{Ch1}^{\bullet-}$ ) that is lower in energy than  $^1\text{Ch1}^*$ . Formation of  $\text{I}^{\bullet+}$  results in bond lengthening, which is a mechanism for nonradiative energy dissipation. Quenching requires zeaxanthin, a pigment-binding protein PsbS, and low pH in the thylakoid lumen. A combination of low pH and excess light activates the xanthophyll cycle through the enzyme violaxanthin deepoxidase, which drives deep oxidation of violaxanthin to zeaxanthin. Also a low thylakoid lumen pH activates binding of zeaxanthin to PsbS by protonating carboxylate chains of violaxanthin deepoxidase and PsbS, thus facilitating attachment to the membrane and the conversion of violaxanthin to zeaxanthin. The low pH also drives adenosine triphosphate synthesis.

## Proteomic Analysis of the *Salmonella enterica* Subspecies serovar *Typhimurium* Isolated from RAW 264.7 Macrophages: Identification of a Novel Protein that Contributes to the Replication of *s. Typhimurium* Inside Macrophages

L Shi,<sup>(a)</sup> JN Adkins,<sup>(a)</sup> JR Coleman,<sup>(a)</sup> AA Schepmoes,<sup>(a)</sup> A Dohnkalkova,<sup>(b)</sup> HM Mottaz,<sup>(b)</sup> AD Norbeck,<sup>(a)</sup> SO Purvine,<sup>(b)</sup> NP Manes,<sup>(a)</sup> HS Smallwood,<sup>(a)</sup> H Wang,<sup>(a)</sup> J Forbes,<sup>(c)</sup> P Gros,<sup>(c)</sup> S Uzzau,<sup>(d)</sup> KD Rodland,<sup>(a)</sup> F Heffron,<sup>(e)</sup> RD Smith,<sup>(a)</sup> and TC Squier<sup>(a)</sup>

(a) Pacific Northwest National Laboratory, Richland, Washington

(b) W.R. Wiley Environmental Molecular Sciences Laboratory, Richland, Washington

(c) McGill University, Montreal, Quebec, Canada

(d) University of Sassari, 07100 Sassari, Italy

(e) Oregon Health Sciences University, Portland, Oregon

The pathogen *Salmonella enterica* is known to cause both food poisoning and typhoid fever. Because of the emergence of antibiotic-resistant isolates and the threat of bioterrorism (e.g., through contamination of food supplies), there is a growing need to study this bacterium.

In this study, a comparative peptidomics approach was used to study the *Salmonella enterica* subspecies serovar *Typhimurium* cultured under four conditions: 1) rapid growth in rich medium, 2) a stationary phase sustained in nutrient-depleted medium, and 3) short-term and 4) long-term exposure to an acidic, low-magnesium, minimal-nutrient medium designed to mimic the macrophage phagosomal environment within which *Salmonella* are known to survive. Native peptides from cleared cell lysates were enriched by isopropanol extraction and analyzed by liquid chromatography-mass spectrometry (LC-MS) and the accurate mass and time (AMT) tag approach. We identified and quantified 5163 peptides originating from 682 proteins, and the data clearly indicated that *Salmonella* exposed to the phagosome-mimicking medium had relatively high abundances of a wide variety of protein degradation products, especially from ribosomal proteins. The same *Salmonella* samples also were analyzed using traditional bottom-up proteomic methods, and when the peptidomic and proteomic data were analyzed together using a hierarchical cluster analysis, two clusters, putative growth proteins (Gr.P.) and putative stress response factors (S.R.F.), of proteins targeted for proteolysis were identified (see Figure 1).

Each column in Figure 1 corresponds to the sample analyzed by LC-MS, and each row represents an individual protein (278 total). All of the data were simultaneously clustered, and the abundance values are indicated by the color bar at the bottom of the figure. The two protein clusters are indicated, and the four culture conditions are designated as follows:

1. L – Rapid growth in rich medium
2. S – Stationary phase in nutrient depleted medium
3. M – Short-term exposure to phagosome-mimicking medium
4. N – Long-term exposure to phagosome-mimicking medium.

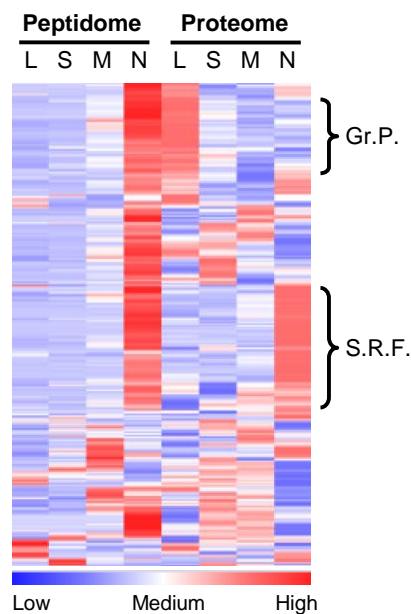


**Figure 1.** Peptidomic and proteomic co-cluster analysis.

The Gr.P. cluster consisted of 48 proteins that were highly abundant in rapidly growing Salmonella and highly fragmented in cells exposed to the phagosome-mimicking medium. Almost all of these proteins (i.e., 37 of 48) were ribosomal proteins, which correlates well with a catabolic pathway known to be activated in Salmonella during stressful conditions and to target ribosomes.

The S.R.F. cluster consisted of 71 proteins that were both highly abundant and highly fragmented in cells exposed to the phagosome-mimicking medium. That Salmonella would up-regulate the expression of stress response factors only to target them for degradation is seemingly paradoxical. However, translational fidelity is known to dramatically decrease during stress, which results in mistranslated proteins that are significantly less likely to properly fold; consequently, their exposure to proteolysis is increased. Therefore, two modes of protein degradation are likely up-regulated by phagocytosed Salmonella: 1) catabolism of ribosomal proteins and 2) proteolysis of defective stress response factors.

These results led to the hypothesis that the Lon protease targets ribosomal proteins for degradation in phagocytosed Salmonella. To investigate this hypothesis, both wild-type and Lon *s. Typhimurium* were cultured in both rich and phagosome-mimicking media, and their peptidomes were analyzed using the AMT tag approach. A preliminary analysis of the resulting data indicated, surprisingly, that knocking out Lon actually resulted in an increase in ribosomal protein degradation, as well as a number of other effects.

## Synthesis and Characterization of Lithium-Doped Tin Dioxide Nanocrystalline Powders

**A Chaparadza,<sup>(a)</sup> SB Ranavare,<sup>(a)</sup> and V Shutthanandan<sup>(b)</sup>**

**(a) Portland State University, Portland, Oregon**

**(b) W.R. Wiley Environmental Molecular Sciences Laboratory, Richland, Washington**

*Flat panel liquid crystal displays use degenerated doped indium tin oxide as conductive electrodes, but thin film based transistors on silicon are needed for addressing individual pixels. Processing of silicon thin film transistors increases the cost of fabrication for large-area displays. However, if highly conductive p-type tin oxide ( $\text{SnO}_2$ ) can be realized, oxide-based inexpensive transistors can dramatically alter the production cost and ease material processing. Currently, the “unipolar” doping problem of  $\text{SnO}_2$  has been an obstacle. In this research, we examined the prospects of effective p-doping of  $\text{SnO}_2$  using lithium as a dopant.*

Several structural and functional phenomena in materials science are directly related to particle size. In recent years, studies of nanometer-sized materials have characterized the effects of finite size on thermodynamic and quantum mechanical properties, leading to novel catalytic, optical, and electronic applications. In this regard, corrosion-resistant, tin-oxide ( $\text{SnO}_2$ ) nanoparticles have important niche applications. Some well-known examples include solar energy conversion, catalysis, gas sensing, antistatic coating, and transparent electrode preparations. Another potential application of  $\text{SnO}_2$  is for transparent electronics, which would be especially valuable in flat panel liquid crystal displays (LCDs) that already use degenerated-doped indium  $\text{SnO}_2$  as conductive electrodes, but need thin film transistors (TFTs) based on silicon for addressing individual pixels. Processing of silicon TFTs increases the cost of fabrication of large-area displays. However, if highly conductive p-type  $\text{SnO}_2$  can be realized, inexpensive oxide-based transistors could dramatically alter the production cost and ease material processing. Currently, the “unipolar” doping problem of  $\text{SnO}_2$  has been an obstacle. There are only a few examples of p-doped  $\text{SnO}_2$ . Theoretically, if effective substitution of tin (Sn) with III-family elements [e.g., cesium (Ce)] or substitution with lithium (Li) is realized, then p-type  $\text{SnO}_2$  could be synthesized.

In this paper, we examine the prospects of effective p-doping of  $\text{SnO}_2$  using Li as a dopant. Pure and Li-doped  $\text{SnO}_2$  nanoparticles were synthesized using the sol-gel precipitation method in the presence of LiCl. There were several potential complications in Li doping  $\text{SnO}_2$  especially at high dopant concentration. First, high Li concentration might lead to formation of lithium stannate ( $\text{Li}_2\text{SnO}_3$ ), which would effectively phase

separate during commonly used high-calcination temperatures. We used a combination of nuclear reaction analysis (NRA) and high-resolution transmission electron microscopy (TEM) studies to probe this possibility. Second, the nature of  $\alpha$  or  $\beta$  stannic acid, especially its degree of ionization, might influence whether or not Li is incorporated in the cassiterite lattice of  $\text{SnO}_2$ . We employed a wide range of pH conditions during the synthesis to affect the oxo-ionic acid charge. Finally, under these varied reaction conditions, we anticipated that the particle size, particle crystallinity, and occurrence of additional crystalline phases might be influenced. We employed x-ray diffraction (XRD) analysis to quantify these effects. The precipitation pH was found to play an important role when it comes to Li doping. Nuclear reaction analysis (NRA) showed that Li is not detected (i.e.,  $<0.005$  atomic-percent level) when the solution pH during synthesis is less than 7, while above pH of 7, relatively small amounts of Li are incorporated. Doping level does not appear to alter the lattice structure of cassiterite. The XRD patterns of the undoped and doped  $\text{SnO}_2$  in Figure 1 show only the tetragonal rutile structure. These results agree with results obtained in earlier work, and at least at the level of doping and processing conditions, we were unable to detect measurable quantities of crystalline  $\text{Li}_2\text{SnO}_3$ .

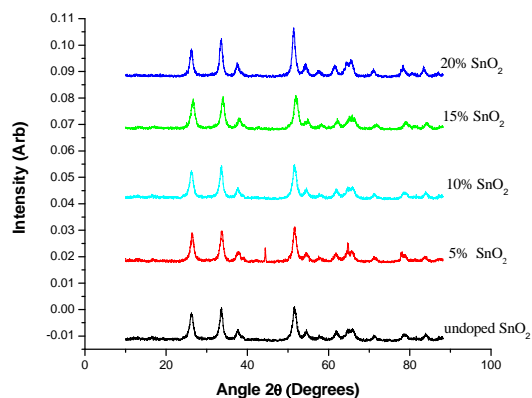


**Figure 1.** XRD patterns of Li-doped  $\text{SnO}_2$  (numbers indicate the percent of LiCl during synthesis).

The crystallite size as determined from XRD analysis decreases with increasing concentration of LiCl used during doping. It is evident from this study that it is possible to control particle size by controlling the LiCl concentration. Although high concentrations of LiCl are used during synthesis, the concentration of dopant Li incorporated is small, as determined by NRA. Therefore, we plotted the particle size data as a function of Li incorporated and found that it varies inversely with Li concentration. Although NRA data provide the amount of Li, it does not reveal the spatial distribution of Li within nanoparticles. At higher Li doping levels, a chemical complexity may arise because of solid-solid phase separation of conductive amorphous or a thin shell of  $\text{Li}_2\text{SnO}_3$  from  $\text{SnO}_2$ . To study this possibility, we considered a crude shell model in which an outer amorphous shell of  $\text{Li}_2\text{SnO}_3$  surrounds the undoped  $\text{SnO}_2$ . Using a simple mass balance consideration, the shell model expression can be derived. In the model depicted in Figure 2, the shell thickness depends on the concentration of the Li incorporated in the cassiterite structure (i.e., the bulk of the nanoparticles). Here we assumed shell thickness was zero. As more Li dissolves in the lattice, the thinner the shell becomes. Because we were unable to locate any diffraction peaks within the sensitivity of our x-ray instrument, we conducted search of such thin shell using high-resolution TEM.

The data in Figure 3 allow us to bound the thickness of the amorphous layer at about 0.2 nm. Thus, combined XRD, TEM, and NRA data imply a very thin shell and minimal solubility of Li in the  $\text{SnO}_2$  lattice. Recently, we verified the phase-separation model described above using Li-nuclear magnetic resonance studies that

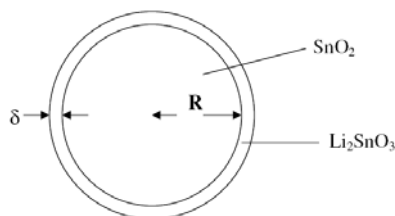


**Figure 2.** Shell model.

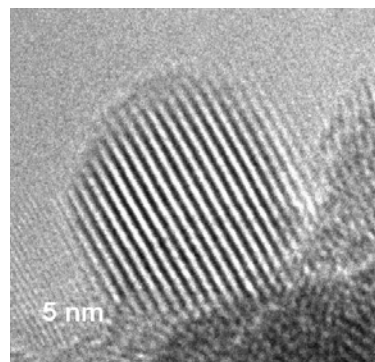


**Figure 3.** High-resolution TEM image of 15 percent Li doped  $\text{SnO}_2$ .

revealed two component spectra—one isotropic peak indicating tetrahedral symmetry (for Li dissolved in bulk) and another axially symmetric powder pattern for the surface-bound Li. The latter spectrum exhibited non-zero quadrupolar splitting.

Nanoscale phase separation, as indicated in our studies, has some interesting consequences for device design. Lithium is believed to convert n-type  $\text{SnO}_x$  to p-type  $\text{SnO}_x$ . However to bring about such carrier inversion, intrinsic n-doping resulting from oxygen vacancies must be overcome. Given the high n-type carrier density in  $\text{SnO}_x$ , a significant concentration of p-type dopant must be introduced in the lattice. Our studies indicate that at a carrier density of approximately  $10^{21} \text{ cm}^{-3}$ , about 0.16 atomic-percent of Li can be accommodated. However, a substantial fraction of Li remains on the surface, thus reducing the extent of bulk p-type doping. The observed Li concentration dependence of p-doping in  $\text{SnO}_x$  by other researchers indicates that increasing the concentration of LiCl in synthesis above 15 percent leads to a reduction in the p-type carrier density. This is consistent with the simple phase-separation model presented above. In conclusion, a sol-precipitation method was used to prepare  $\text{SnO}_2$  and Li-doped nanoparticles. From this work, we managed to show that Li-insertion into  $\text{SnO}_2$  is pH dependent and only occurs under alkaline conditions. By varying pH, temperature, and dopant level, we demonstrated that it is possible to control the nanoparticle size. Low particle growth rates were obtained by the introduction of Li particles into the  $\text{SnO}_2$ .

## Awards and Recognition

L-S Wang, Washington State University Tri-Cities, was awarded the Sahlin Faculty Excellence Award for Research, Scholarship, and Arts from Washington State University. The university presents three Sahlin awards each year to recognize excellence in teaching, public service, and research.



L-S Wang

## Professional/Community Service

Eleven Washington State University students enrolled in the Organic Qualitative Analysis Laboratory and two of their instructors visited EMSL on March 27, 2007. The visit included a practical nuclear magnetic resonance (NMR) demonstration during which the students had  $^1\text{H}$  spectra recorded to identify the different products purified from one of their organic synthesis experiments.

The visit also included tours of both the High-Field Magnetic Resonance Facility and the High-Performance Mass Spectrometry Facility where the hosts J Ford and H Udseth covered instrument details that would enable the scientists to address various science problems. SD Burton worked with the students to collect data from their samples. All the visitors found the practical demonstration and tours valuable for understanding what expertise and facilities support their research.





Washington State University students and instructors who visited EMSL on March 27, 2007

## Visitors and Users

During this reporting period, a total of 355 users benefited from EMSL capabilities and expertise. This total included 168 onsite users and 187 remote users.

## New EMSL Staff

DR Sisk accepted the Group Leader position for EMSL's Instrument Development Laboratory in March. He transferred to EMSL from the Radiation and Health Technology Group in PNNL's Environmental Technology Directorate. He has a B.S. in Physics and an M.S. in Electrical Engineering. He has many years of instrument-development experience at PNNL, including providing key support in the development of a detection and measurement system used to measure radiation at the Chernobyl Nuclear Power Plant in Ukraine, and ample experience in managing multidisciplinary teams supporting systems-level solutions.

## Publications

Baer DR. 2007. “Improving Surface-Analysis Methods for Characterization of Advanced Materials by Development of Standards, Reference Data, and Interlaboratory Comparisons.” *Surface and Interface Analysis* 39(4):283-293. DOI: 10.1002/sia.2508.

Belov ME, MA Buschbach, DC Prior, K Tang, and RD Smith. 2007. “Multiplexed Ion Mobility Spectrometry-Orthogonal Time-of-Flight Mass Spectrometry.” *Analytical Chemistry* 79(6):2451-2462. DOI: 10.1021/ac0617316.

Brooks KP, J Hu, H Zhu, and R Kee. 2007. “Methanation of Carbon Dioxide by Hydrogen Reduction Using the Sabatier Process in Microchannel Reactors.” *Chemical Engineering Science* 62(4):1161-1170. DOI: 10.1016/j.ces.2006.11.020.

Chaparadza A, SB Rananavare, and V Shutthanandan. 2007. “Synthesis and Characterization of Lithium-Doped Tin Dioxide Nanocrystalline Powders.” *Materials Chemistry and Physics* 102(2-3):176-180. DOI: 10.1016/j.matchemphys.2006.11.022.

Cheung SH, P Nachimuthu, AG Joly, MH Engelhard, MK Bowman, and SA Chambers. 2007. “N Incorporation and Electronic Structure in N-Doped TiO<sub>2</sub>(110) Rutile.” *Surface Science* 601(7):1754-1762. DOI: 10.1016/j.susc.2007.01.051.

Conrad BR, WG Cullen, DB Dougherty, L Lyubinetsky, and ED Williams. 2007. “Spatial First-Passage Statistics of Al/Si(111)-(√3√3)/Step Fluctuations.” *Physical Review E* 75(2): Art. No. 021603.

Cui L, X Huang, L Wang, J Li, and LS Wang. 2007. “Endohedral Stannaspherenes M@Sn<sub>12</sub>: A Rich Class of Stable Molecular Cage Clusters.” *Angewandte Chemie International Edition* 46(5):742-745. DOI: 10.1002/anie.200603226.

Dantas G, C Corrent, SL Reichow, JJ Havranek, ZM Eletr, NG Isern, B Kuhlman, G Varani, EA Merritt, and D Baker. 2007. “High-Resolution Structural and Thermodynamic Analysis of Extreme Stabilization of Human Procarboxypeptidase by Computational Protein Design.” *Journal of Molecular Biology* 366(4):1209-1221. DOI: 10.1016/j.jmb.2006.11.080.

Devanathan R, F Gao, and WJ Weber. 2007. “Atomistic Modeling of Amorphous Silicon Carbide Using a Bond-Order Potential.” *Nuclear Instruments and Methods in Physics Research. Section B, Beam Interactions with Materials and Atoms* 255(1):130-135. DOI: 10.1016/j.nimb.2006.11.045.

Devanathan R, P Durham, J Du, LR Corrales, and EM Bringa. 2007. “Molecular Dynamics Simulation of Amorphization in Forsterite by Cosmic Rays.” *Nuclear Instruments and Methods in Physics Research. Section B, Beam Interactions with Materials and Atoms* 255(1):172-176. DOI: 10.1016/j.nimb.2006.11.021.

Ding S, W Qian, and RD Smith. 2007. “Quantitative Proteomic Approaches for Studying Phosphotyrosine Signaling.” *Expert Review of Proteomics* 4(1):13-23. DOI: 10.1586/14789450.4.1.13.

Elias DA, F Yang, HM Mottaz, AS Beliaev, and MS Lipton. 2007. “Enrichment of Functional Redox Reactive Proteins and Identification by Mass Spectrometry Results in Several Terminal Fe(III)-Reducing Candidate Proteins in *Shewanella oneidensis* MR-1.” *Journal of Microbiological Methods* 68(2):367-375. DOI: 10.1016/j.mimet.2006.09.023.

Farber R. 2007. "HPC Valance and Common Sense." *Scientific Computing*. Accessed May 22, 2007, at <http://www.scientificcomputing.com/ShowPR.aspx?PUBCODE=030&ACCT=3000000100&ISSUE=0702&RELTYPE=PR&ORIGRELTYPE=HPCC&PRODCODE=00000000&PRODLETT=E>.

Flaherty DW, Z Dohnalek, A Dohnalkova, BW Arey, DE McCready, N Ponnusamy, C Mullins, and BD Kay. 2007. "Reactive Ballistic Deposition of Porous TiO<sub>2</sub> Films: Growth and Characterization." *Journal of Physical Chemistry C* 111(12):4765-4773. DOI: 10.1021/jp067641m.

Gao F, LW Campbell, R Devanathan, Y Xie, Y Zhang, AJ Peurrung, and WJ Weber. 2007. "Gamma-Ray Interaction in Ge: A Monte Carlo Simulation." *Nuclear Instruments and Methods in Physics Research. Section B, Beam Interactions with Materials and Atoms* 255(1):286-290. DOI: 10.1016/j.nimb.2006.11.031.

Gao F, Y Zhang, R Devanathan, M Posselt, and WJ Weber. 2007. "Atomistic Simulations of Epitaxial Recrystallization in 4H-SiC Along the [0001] Direction." *Nuclear Instruments and Methods in Physics Research. Section B, Beam Interactions with Materials and Atoms* 255(1):136-140. DOI: 10.1016/j.nimb.2006.11.016.

Gibbs GV, DF Cox, KM Rosso, NL Ross, RT Downs, and MA Spackman. 2007. "Theoretical Electron Density Distributions for Fe- and Cu-Sulfide Earth Materials: A Connection between Bond Length, Bond Critical Point Properties, Local Energy Densities, and Bonded Interactions." *Journal of Physical Chemistry B* 111(8):1923-1931. DOI: 10.1021/jp065086i.

Groenewold GS, AK Gianotto, KC Cossel, MJ Van Stipdonk, J Oomens, N Polfer, DT Moore, WA de Jong, and ME McIlwain. 2007. "Mid-Infrared Vibrational Spectra of Discrete Acetone-Ligated Cerium Hydroxide Cations." *Physical Chemistry Chemical Physics PCCP* 9(5):596-606. DOI: 10.1039/b613029a.

Haranczyk M and MS Gutowski. 2007. "Differences in Electrostatic Potential Around DNA Fragments Containing Guanine and 8-oxo-Guanine." *Theoretical Chemistry Accounts* 117(2):291-296. DOI: 10.1007/s00214-006-0133-1.

Joly AG, G Xiong, CM Wang, DE McCready, KM Beck, and WP Hess. 2007. "Synthesis and Photoexcited Charge Carrier Dynamics of  $\beta$ -FeOOH Nanorods." *Applied Physics Letters* 90(10):103504. DOI: 10.1063/1.2711395.

Kim J, O Bondarchuk, BD Kay, JM White, and Z Dohnalek. 2007. "Preparation and Characterization of Monodispersed WO<sub>3</sub> Nanoclusters on TiO<sub>2</sub>(110)." *Catalysis Today* 120(2):186-195. DOI: 10.1016/j.cattod.2006.07.050.

Kim M, J Kim, J Lee, H Jia, H Na, J Youn, J Kwak, A Dohnalkova, JW Grate, P Wang, T Hyeon, H Park, and H Chang. 2007. "Crosslinked Enzyme Aggregates in Hierarchically-Ordered Mesoporous Silica: A Simple and Effective Method for Enzyme Stabilization." *Biotechnology and Bioengineering* 96(2):210-218. DOI: 10.1002/bit.21107.

Li J, SM Kathmann, GK Schenter, and M Gutowski. 2007. "Isomers and Conformers of H(NH<sub>2</sub>BH<sub>2</sub>)<sub>n</sub>H Oligomers: Understanding the Geometries and Electronic Structure of Boron-Nitrogen-Hydrogen Compounds as Potential Hydrogen Storage Materials." *Journal of Physical Chemistry C* 111(8):3294-3299. DOI: 10.1021/jp066360b.

Li XS, GE Fryxell, CM Wang, and J Young. 2007. "Templating Mesoporous Hierarchies in Silica Thin Films Using the Thermal Degradation of Cellulose Nitrate." *Microporous and Mesoporous Materials* 99(3):308-318. DOI: 10.1016/j.micromeso.2006.09.037.

- Mazurkiewicz K, M Haranczyk, M Gutowski, J Rak, D Radisic, SN Esutis, D Wang, and KH Bowen. 2007. "Valence Anions in Complexes of Adenine and 9-Methyladenine with Formic Acid: Stabilization by Intermolecular Proton Transfer." *Journal of the American Chemical Society* 129(5):1216-1224. DOI: 10.1021/ja066229h.
- Morgan WF and MB Sowa. 2007. "Non-Targeted Bystander Effects Induced by Ionizing Radiation." *Mutation Research/Fundamental and Molecular Mechanisms of Mutagenesis* 616(1-2):159-164.
- Ostrom M, MJ Truex, PD Thorne, and TW Wietsma. 2007. "Three-Dimensional Multifluid Flow and Transport at the Brooklawn Site near Baton Rouge, LA: A Case Study." *Soil & Sediment Contamination* 16(2):109-141.
- Ostrom M, TW Wietsma, MA Covert, and VR Vermeul. 2007. "Zero-Valent Iron Emplacement in Permeable Porous Media Using Polymer Additions." *Ground Water Monitoring and Remediation* 27(1):122-130.
- Ramelot TA, A Yee, JR Cort, A Semesi, CH Arrowsmith, and MA Kennedy. 2007. "NMR Structure and Binding Studies Confirm that PA4608 from *Pseudomonas aeruginosa* is a PilZ Domain and a c-di-GMP Binding Protein." *Proteins: Structure, Function, and Bioinformatics* 66(2):266-271. DOI: 10.1002/prot.21199.
- Resch W, KK Hixson, RJ Moore, MS Lipton, and B Moss. 2007. "Protein Composition of the Vaccinia Virus Mature Virion." *Virology* 358(1):233-247.
- Schlag EW, S Sheu, D Yang, HL Selzle, and S Lin. 2007. "Distal Charge Transport in Peptides." *Angewandte Chemie International Edition* 46(18):3196-3210. DOI: 10.1002/anie.200601623.
- Sharma S, DC Simpson, N Tolic, N Jaitly, AM Mayampurath, RD Smith, and L Pasa-Tolic. 2007. "Proteomic Profiling of Intact Proteins Using WAX-RPLC 2-D Separations and FTICR Mass Spectrometry." *Journal of Proteome Research* 6(2):602-610.
- Shvartsburg AA, F Li, K Tang, and RD Smith. 2007. "Distortion of Ion Structures by Field Asymmetric Waveform Ion Mobility Spectrometry." *Analytical Chemistry* 79(4):1523-1528. DOI: 10.1021/ac061306c.
- Timchalk C, JA Campbell, G Liu, Y Lin, and AA Kousba. 2007. "Development of a Non-Invasive Biomonitoring Approach to Determine Exposure to the Organophosphorus Insecticide Chlorpyrifos in Rat Saliva." *Toxicology and Applied Pharmacology* 219(2-3):217-225. DOI: 10.1016/j.taap.2006.10.002.
- Verma S, Y Xiong, MU Mayer, and TC Squier. 2007. "Remodeling of Bacterial RNA Polymerase Supramolecular Complex in Response to Environmental Conditions." *Biochemistry* 46(11):3023-3035.
- Wang Z, X Zu, F Gao, and WJ Weber. 2007. "Atomistic Study of the Melting Behavior of Single Crystalline Wurtzite Gallium Nitride Nanowires." *Journal of Materials Research* 22(3):742-747. DOI: 10.1557/JMR.2007.0095.
- Wang Z, X Zu, F Gao, and WJ Weber. 2007. "Size Dependence of Melting of GaN Nanowires with Triangular Cross Sections." *Journal of Applied Physics* 101(4):043511. DOI: 10.1063/1.2512140.
- Wei W, SL Parker, Y Sun, JM White, G Xiong, AG Joly, KM Beck, and WP Hess. 2007. "Study of Copper Diffusion through a Ruthenium Thin Film by Photoemission Electron Microscopy." *Applied Physics Letters* 90(11): Art. No. 111906.

Wellman DM, SV Mattigod, BW Arey, MI Wood, and SW Forrester. 2007. “Experimental Limitations Regarding the Formation and Characterization of Uranium-Mineral Phases in Concrete Waste Forms.” *Cement and Concrete Research* 37(2):151-160.

Whiteaker JR, H Zhang, JK Eng, R Fang, BD Piening, L Feng, TD Lorentzen, RM Schoenherr, JF Keane, T Holzman, M Fitzgibbon, C Lin, H Zhang, K Cooke, T Liu, DG Camp, II, LN Anderson, J Watts, RD Smith, M McIntosh, and AG Paulovich. 2007. “Head-to-Head Comparison of Serum Fractionation Techniques.” *Journal of Proteome Research* 6(2):828-836. DOI: 10.1021/pr0604920.

Wigginton NS, KM Rosso, BH Lower, L Shi, and MF Hochella. 2007. “Electron Tunneling Properties of Outer-Membrane Decaheme Cytochromes from *Shewanella oneidensis*.” *Geochimica et Cosmochimica Acta* 71(3):543-555.

Williams SD, TJ Johnson, T Gibbons, and CL Kitchens. 2007. “Relative Raman Intensities in C<sub>6</sub>H<sub>6</sub>, C<sub>6</sub>D<sub>6</sub>, and C<sub>6</sub>F<sub>6</sub>: A Comparison of Different Computational Methods.” *Theoretical Chemistry Accounts* 117(2): 283-290. DOI: 10.1007/s00214-006-1350-z.

Xiong G, AG Joly, KM Beck, and WP Hess. 2007. “Laser-Induced Oxygen Vacancy Formation and Diffusion on TiO<sub>2</sub>(110) Surfaces Probed by Photoemission Electron Microscopy.” *Physica Status Solidi C* 3(10):3598-3602.

Yakovkin IN and MS Gutowski. 2007. “Driving Force for the WO<sub>3</sub>(001) Surface Relaxation.” *Surface Science* 601(6):1481-1488. DOI: 10.1016/j.susc.2007.01.013.

Yongsunthon R, V Fowler, Jr., BH Lower, FP Vellano, E Alexander, L Reller, G Corey, and SK Lower. 2007. “Correlation between Fundamental Binding Forces and Clinical Prognosis of *Staphylococcus aureus* Infections of Medical Implants.” *Langmuir* 23(5):2289-2292.

Yu Z, CM Wang, MH Engelhard, P Nachimuthu, DE McCready, IV Lyubinetsky, and S Thevuthasan. 2007. “Epitaxial Growth and Microstructure of Cu<sub>2</sub>O Nanoparticle/Thin Films on SrTiO<sub>3</sub>(100).” *Nanotechnology* 18(11): Art. No. 115601. DOI: 10.1088/0957-4484/18/11/115601.

Zachara JM, SM Heald, B Jeon, RK Kukkadapu, C Liu, JP McKinley, A Dohnalkova, and DA Moore. 2007. “Reduction of Per technetate [Tc(VII)] by Aqueous Fe(II) and the Nature of Solid Phase Redox Products.” *Geochimica et Cosmochimica Acta* 71(9):2137-2157. DOI: 10.1016/j.gca.2006.10.025.

Zelenyuk AN and DG Imre. 2007. “On the Effect of Particle Alignment in the DMA.” *Aerosol Science and Technology* 41(2):112-124. DOI: 10.1080/02786820601118380.

Zhang Q, A Frolov, N Tang, R Hoffman, T van der Goor, T Metz, and RD Smith. 2007. “Application of Electron Transfer Dissociation Mass Spectrometry in Analyses of Non-Enzymatically Glycated Peptides.” *Rapid Communications in Mass Spectrometry* 21(5):661-666. DOI: 10.1002/rcm.2884.

Zhao H, J Kwak, C Zhang, HM Brown, BW Arey, and JE Holladay. 2007. “Studying Cellulose Fiber Structure by SEM, XRD, NMR, and Acid Hydrolysis.” *Carbohydrate Polymers* 68(2):235-241.

Zubarev DY, AI Boldyrev, J Li, H Zhai, and LS Wang. 2007. “On the Chemical Bonding of Gold in Auro-Boron Oxide Clusters Au<sub>n</sub>BO-(n=1-3).” *Journal of Physical Chemistry A* 111(9):1648-1658. DOI: 10.1021/jp0657437.

Zubatyyuk RI, YM Volovenko, O Shishkin, L Gorb, and J Leszczynski. 2007. “Aromaticity-Controlled Tautomerism and Resonance-Assisted Hydrogen Bonding in Heterocyclic Enaminone-Iminoenol Systems.” *Journal of Organic Chemistry* 72(3):725-735. DOI: 10.1021/jo0616411.

## Presentations

*During this reporting period, EMSL staff presented on research performed at the user facility at the following meetings or locations:*

- Seminar presentation of an experimental study of electronic stopping power in compounds, February 16, 2007, University of Michigan, Ann Arbor, Michigan.
- 2007 SIAM Conference on Computational Science and Engineering, February 19, 2007, Costa Mesa, California.
- Gordon Conference on Gaseous Ions: Structures, Energetics, and Reactions, February 25-March 2, 2007, Ventura, California.
- American Physical Society 2007 March Meeting, March 5-9, 2007, Denver, Colorado.
- Mouse 1,2,3,4-diepoxybutane (BDI) and Clinical Proteomic Technology Assessment for Cancer (CPTAC) Team Meeting, March 9, 2007, Seattle, Washington.
- Safer Nano 2007 Conference, March 12-13, 2007, Eugene, Oregon.
- American Chemical Society National Meeting and Exposition, March 23-29, 2007, Chicago, Illinois.
- Society of Toxicology 46<sup>th</sup> Annual Meeting and ToxExpo, March 25-April 1, 2007, Charlotte, North Carolina.